

CHAPTER II

CONFINEMENT AND REINFORCEMENT BUCKLING MODELS

2.1 Confinement Model with Consideration of Concrete core-Transverse Steel Interaction

The characteristic of confined concrete is one of the most interesting research topics during the last two decades. Unlike the confinement provided by active hydrostatic pressure, it is well known that the confinement pressure in a reinforced concrete (RC) column is passive in nature and varies along the height of the column and over the cross-section of the concrete core. Under the applied axial strain, the level of stress in the transverse steel, which produces the passive confining pressure, depends on the amount of lateral expansion on the concrete core, and the flexibilities of the transverse steel. Therefore, in order to accurately predict the behavior of confined RC columns, the interaction between the deformation of the concrete core and transverse steel must be considered.

This study presents an alternative rational procedure for determining the strength enhancement of both normal- and high-strength RC columns under uniaxial vertical loading, taking into account the interaction between the concrete core and transverse steel and the variation of confining stress along the height of the column. The effect of flexibility of perimeter ties is directly included in this study. The proposed approach has the advantage that one can obtain the effective confining pressure directly from mechanics principles rather than from regression analyses of test results or from the concept of an effectively confined area which have more limitations in application. Buckling of longitudinal bars is not considered in this stage of formulation.

2.1.1 The Concept

Figure 2.1 shows a RC column with hoops spaced vertically at spacing of s . Under a uniform axial strain, the core would expand uniformly [as shown in dashed lines in Figure 2.1(b)] if there were no hoops confining the core. The lateral expansion

of the core stretches and bends the hoop, resulting in interactive line forces at the hoop positions as depicted in Figures 2.2(a) and 2.2(b). The interactive forces produce a non-linear confining pressure along the height as shown in Figure 2.3. Results from three-dimensional finite element analyses of an elastic concrete core bound by elastic hoops are used to obtain simple relations for the variation of confining stress over the vertical hoop spacing and the confining force transferred by the perimeter ties. The equilibrium condition is invoked on the effective stress resultant in the concrete and the axial forces in the ties. The concept of area compatibility is employed to ensure compatibility of the concrete core and steel hoop in a global sense. The condition of zero volumetric strain is used to specify the state at which the concrete attains the peak compressive strength. Due to the non-linear nature of concrete behavior, an iterative procedure is needed in the computation. As suggested by Imran and Pantazopoulou (1996), the resulting axial stress with the influence of confinement is then obtained using the well known Richart model [Richart et al. (1928)].

2.1.2 Relationships between Peak and Average Stresses and Strains

As mentioned earlier, under the applied axial strain, the concrete core expands and induces interactive confining forces between the concrete core and the hoops. The interactive forces produce non-linear confining stresses over the cross-section and along the vertical direction. The determination of the strength of concrete under triaxial stress state involves a three-dimensional (3-D) problem, which is difficult to solve theoretically.

In order to transform the complicated 3-D problem to a 2-D one, a 3-D finite element model is utilized to determine the effective confining stress at the hoop level, $\sigma_{h,eff}$, the average effective confining stress, σ_{eff} , the interactive line forces acting on the hoop as well as the area strains averaged over the cross-sectional area at the hoop level, $\varepsilon_{A,h}$, and the average area strain over the column height, $\varepsilon_{A,ave}$. First, the effective confining stress at any level z is defined [Mau et al. (1998)]:

$$\sigma_{eff}(z) = \frac{1}{A} \int_A \frac{(\sigma_x + \sigma_y)}{2} dA \quad (2.1)$$

where σ_x and σ_y are the stresses in the x and y directions, respectively, and A is the area of the concrete core. In this study, compressive stresses and strains are assigned negative values.

In the finite element modeling, the concrete core is modeled using 8-node brick elements, while the perimeter tie is discretized as beam elements. In addition, rigid truss elements are used to capture the interactive forces between the concrete core and the perimeter ties. Based on the results from 3-D finite element analyses shown in Figures 2.4(a) and 2.4(b), the following relations are obtained by simple regression:

$$\frac{\sigma_{h,eff}}{\sigma_{eff}} = 1 + 3.1342 \frac{s}{B'_c} \quad (2.2)$$

$$\varepsilon_{A,ave} - \varepsilon_{A,h} = \frac{2(1 - \nu_e)(\sigma_{eff} - \sigma_{h,eff})}{E_c} \quad (2.3)$$

in which s and B'_c are, respectively, the hoop spacing and the clear distance between the two longitudinal bars at the corners of the hoop [as shown in Figure 2.2(b)], and ν_e is the equivalent Poisson's ratio, as shown in Appendix A, corresponding to the level of expansion of concrete which can be determined from the following relation:

$$\nu_e = \frac{\left(\frac{\Delta\sigma_{eff}}{E_c} - \frac{\Delta\varepsilon_{A,ave}}{2} \right)}{\left(\frac{\Delta\sigma_{eff}}{E_c} + \Delta\varepsilon_z \right)} \quad (2.4)$$

where ε_z is the applied axial strain, Δ denotes the incremental quantity, and E_c is the residual elastic stiffness in the concrete core which can be expressed in terms of the initial stiffness, $E_{c,i}$ and the average area strain as follows [Imran and Pantazopoulou (1996)]:

$$\frac{E_c}{E_{c,i}} = \frac{1}{1 + \frac{\varepsilon_{A,ave}}{0.05}} \quad (2.5)$$

2.1.3 Deformation of Concrete under Triaxial Stress State

Pantazopoulou and Mills (1995) illustrated that damage in concrete due to microcracking was manifested by the volumetric expansion of the material. The rate of volume change (i.e. volume increment per unit of initial volume) represents the volumetric strain, ε_v . Partial or total restraint against expansion, usually imposed through the boundary conditions, has a profound influence on the internal stress state of the material.

Under a triaxial stress state, the volumetric strain, ε_v , of the concrete core is given by the following equations [Imran and Pantazopoulou (1996)]:

(a) Prior to cracking in the lateral direction, $\varepsilon_z > \varepsilon_z^{lim}$,

$$\varepsilon_v = (1 - 2\nu_l) \left(\frac{2\sigma_{eff}}{E_c} + \varepsilon_z \right) \quad (2.6)$$

where ε_z^{lim} and ν_l are the axial strain that induces cracking in the lateral direction and initial Poisson's ratio, respectively. The value of ε_z^{lim} is

$$\varepsilon_z^{lim} = \left(\frac{1 - \nu_l}{\nu_l E_c} \right) \sigma_{eff} - \frac{\varepsilon_{cr}}{\nu_l} \quad (2.7)$$

in which ε_{cr} is the cracking strain of concrete in direct tension.

(b) After cracking, $\varepsilon_z < \varepsilon_z^{lim}$,

$$\varepsilon_v = (1 - 2\nu_i) \left\{ \frac{2\sigma_{eff}}{E_c} + \varepsilon'_{cc} \left[\frac{\varepsilon_z}{\varepsilon'_{cc}} - \left(\frac{\varepsilon_z - \varepsilon_z^{lim}}{\varepsilon'_{cc} - \varepsilon_z^{lim}} \right)^2 \right] \right\} \quad (2.8)$$

where ε'_{cc} is the strain at peak confined strength. Subtracting Eq. (2.6) or (2.8) by the applied axial strain, ε_z , results in the average area strain of the concrete core, $\varepsilon_{A,ave}$. As suggested by Imran and Pantazopoulou (1996), ε'_{cc} is related to the peak confined compressive strength, f'_{cc} , by

$$\frac{\varepsilon'_{cc}}{\varepsilon_{co}} = 5 \left[\frac{f'_{cc}}{f'_{co}} - 0.8 \right] \quad (2.9)$$

$$f'_{cc} = f'_{co} + 4.1\sigma_{eff} \quad (2.10)$$

where f'_{co} , and ε_{co} are the unconfined compressive strength and the corresponding strain, respectively. The latter can be approximated from the following equation [Razvi and Saatcioglu (1999)]:

$$\varepsilon_{co} = 0.0028 - 0.0008 \frac{40}{f'_{co}} \quad (2.11)$$

in which f'_{co} is in Megapascals. Referring to the suggestion made by Sheikh and Uzumeri (1982) and Razvi and Saatcioglu (1999) that the strength of the concrete inside the structural member is less than the strength obtained from standard cylinder, f'_c , the value of f'_{co} equals to $0.85f'_c$ is used in this study.

2.1.4 Equilibrium Condition

The global equilibrium of the concrete-tie system can be readily determined from simple statics of the free body shown in Figure 2.5 in which F_h , and F_c are the tensile forces in each perimeter tie and cross-tie, respectively, and F_t is the tensile

force in the concrete cover. The global equilibrium equation can be expressed as follows:

$$2F_h + \sum_{i=1}^N F_c + 2F_t = \sigma_{eff} s B_c \quad (2.12)$$

in which N and B_c are the number of crosstie legs in each direction and the width of the concrete core measured from center-to-center of perimeter tie, respectively. The tensile force in the concrete cover is given by

$$F_t = \sigma_t s t_{cov} \quad (2.13)$$

where σ_t is the tensile stress and t_{cov} is the thickness of the concrete cover. The tensile stress, σ_t , can be determined from the bilinear strain softening relation as a function of the crack width w [Rokugo et al. (1989)] as shown in Figure 2.6. The critical crack width, w_{cr} , can be obtained from the following equation:

$$w_{cr} = \frac{5G_F}{f_t} \quad (2.14)$$

where f_t is the tensile strength and G_F is the fracture energy of concrete.

Results from finite element analyses of elastic core surrounded by perimeter hoop with additional crosstie indicated that the tension in crosstie leg is about 1.7 times the tension in perimeter tie. For simplicity, assuming that tension in a crosstie is two times of that in the perimeter tie for equally spaced tie legs, one can simplify Eq. (2.12) to:

$$F_c = \left(\sigma_{eff} - \frac{2F_t}{sB_c} \right) \left(\frac{B_c}{N+1} \right) s \quad (2.15)$$

$$F_h = \frac{1}{2} \left(\sigma_{eff} - \frac{2F_t}{sB_c} \right) \left(\frac{B_c}{N+1} \right) s \quad (2.16)$$

After concrete cover spalling, the tension in the concrete cover vanishes and the axial force in the perimeter ties and cross-ties can be determined from the above equations by setting F_c equal to zero.

2.1.5 Modeling of Hoop

Due to the flexibility of the hoop under bending, the interactive transverse forces between the concrete core and the hoop vary non-linearly along the tie leg, with much concentration at the corners and at the cross-tie intersections (if cross-ties are provided). Prediction of the transverse interactive force distribution in the tie leg is a very complicated problem. Alternatively, the effect of the interactive transverse forces is assumed to be equivalent to the effect of the resultant forces acting at distances kL from the supports as depicted in Figure 2.7. For ties with Young's modulus, E_s , second moment of inertia, I , and unsupported length, L_s , the parameter k can be estimated from Figure 2.4(c) which is the result of a regression analysis of 3-D finite element solutions of concrete-core-tie systems mentioned earlier.

For simplicity the perimeter tie is modeled as beam elements with the ends fixed, as shown in Figure 2.7. In case the hoop is restrained internally by a cross-tie, the intermediate cross-tie support is also assumed to be restrained against rotation. The assumption of fixed end supports of the hoop is guided by 3-D finite element solutions of the core-tie system which indicate high bending moments developed at the joints of the hoop. Theoretically, such joints should be modeled as rotationally restrained supports. However, for simplicity, the fixed-end support conditions are acceptable in practice. Cross-ties (if provided) are modeled as axial bar elements.

Figure 2.8 shows the free-body diagram of part of the perimeter tie. Neglecting bond between the concrete and hoop after the covering spalls off, and considering equilibrium and symmetry of the hoop under the action of the interactive transverse forces and hoop tension, one may readily show that the resultant of the interactive transverse forces must balance the axial force in the hoop leg in the direction considered. Furthermore, the first two plastic hinges are formed at the fixed

ends. The value of the plastic moment, M_p , is influenced by the presence of the axial force, which can be approximated by the following equation [Chen and Sohal (1995)]:

$$M_p = \frac{d_h^3}{6} f_{yh} \cos\left(\frac{\pi F_h}{2 F_y}\right) \quad (2.17)$$

where d_h , f_{yh} and F_y are the hoop diameter, the yield strength and the yielding force of the perimeter hoop, respectively. The flexural failure mechanism is attained when the final plastic hinge forms at mid-span, as shown in Figure 2.8. Before reaching flexural failure mechanism, the bending deformation of perimeter tie, u_f , can be determined from simple structural analysis. After the flexural failure mechanism is fully developed, the hoop and crosstie (if any) can be further bent and stretched. Beyond this stage, the bending deformation of perimeter tie, u_f , can be determined from the equilibrium condition with consideration of geometrical non-linearity and can be given by the following equation:

$$u_f = kL - \frac{2M_p}{F_h} \quad (2.18)$$

2.1.6 Compatibility of Concrete-tie System

The compatibility of the concrete core and hoop is treated in a global sense. Under bending and stretching, the hoop would expand with an increase in the enclosed area A_h . This can be obtained from the geometry of deformation of perimeter tie, shown in Figure 2.9, as follows:

$$A_h = A_f + A_{a,p} + A_{a,c} \quad (2.19)$$

where A_f and $A_{a,p}$ are the increased areas due to bending deformation, u_f , and uniform expansion of the perimeter tie, $u_{a,p}$, respectively; and $A_{a,c}$ is the increase in area due to elongation of the crosstie, $u_{a,c}$, in excess of that of the hoop in the same direction. Dividing Eq. (2.19) by the undeformed core area yields the area strain of the steel

hoop which has to be equal to that of the concrete core (at the hoop level) as the condition of compatibility.

2.1.7 Procedure for Determining Stress-strain Relation

For a given axial strain, we first assume a trial value of the average effective confining pressure, σ_{eff} . Then, the area strain of the concrete core at the level of the perimeter tie, $\epsilon_{A,h}$, is determined from Eqs. (2.2)-(2.11). With the resultant force of the interactive transverse line load exerted by the core on the tie leg determined from equilibrium, the resulting deformations of the perimeter tie and crosstie (if any) are next computed, and the area strain calculated from the deformation of the ties. If the area strain of the steel hoop is different from the area strain of the concrete core, then iteration is carried out until satisfactory convergence is achieved. These calculation procedures are repeated until the state of zero volumetric strain is reached at which the confined concrete attains the peak confined strength. The associated confining pressure is computed and the confined strength of the concrete core obtained from Eq. (2.10).

2.2 Reinforcement Buckling

In reinforced concrete members, the reinforcing bars might undergo high compressive strain and subject to buckling. Because of the geometrical and material nonlinearities, the average compressive stress carried by the reinforcement decreases in the post-buckling range. However, for reinforcement under tension, no lateral deformation is induced, and hence, the average stress-strain relationship over a finite size of the reinforcement is exactly the same as the pointwise tensile stress-strain relationship.

It has been realized that the onset of buckling of longitudinal reinforcement inside reinforced concrete members is different from buckling of bare reinforcing bars because of the existence of the transverse steels [Papia and Russo (1989), Suda et al. (1996), and Suda and Masukawa (2000)]. Earlier studies by Papia, Russo and Zingone (1988) and Dhakal and Maekawa (2002) show that the transverse steels have major

influence on the initiation of buckling of longitudinal reinforcement inside a reinforced concrete column. In order to model the buckling of longitudinal reinforcement, the average stress-strain relationship proposed by Dhakal (2000) will be used in this study. A typical stress-strain relationship is shown in Figure 2.10. Based on the results from finite element analyses, the average stress-strain relationship for a reinforcement subjected to compressive loading can be determined from the following equations [Dhakal (2000)]:

$$\frac{\sigma}{\sigma_1} = 1 - \left(1 - \frac{\sigma^*}{\sigma_1}\right) \left(\frac{\varepsilon - \varepsilon_y}{\varepsilon^* - \varepsilon_y}\right) \quad \text{for } \varepsilon_y < \varepsilon \leq \varepsilon^* \quad (2.20)$$

$$\sigma = \sigma^* - 0.02E_s(\varepsilon - \varepsilon^*); \quad \sigma \geq 0.2f_y \quad \text{for } \varepsilon > \varepsilon^* \quad (2.21)$$

where σ_1 and σ_1^* are the local stresses corresponding to the current strain, ε , and the strain at intermediate point, ε^* , respectively, f_y and ε_y are the yielding stress and strain, respectively, and E_s is the Young's modulus of the reinforcement. The coordinates of the intermediate point, $(\varepsilon^*, \sigma^*)$, which defines the point after which a constant softening stiffness is assumed to be equal to $0.02E_s$, are given by

$$\frac{\varepsilon^*}{\varepsilon_y} = 55 - 2.3\sqrt{\frac{f_y}{100} \frac{L}{D}}; \quad \frac{\varepsilon^*}{\varepsilon_y} \geq 7 \quad (2.22)$$

$$\frac{\sigma^*}{\sigma_1^*} = \alpha \left(1.1 - 0.016\sqrt{\frac{f_y}{100} \frac{L}{D}}\right); \quad \sigma^* \geq 0.2f_y \quad (2.23)$$

in which L and D are the unsupported length and diameter of the reinforcement, respectively. The coefficient α ranges from 0.75 (for an elasto-plastic material) to 1 (for a material with substantial strain hardening).

The unsupported length, L , can be determined by considering the influence of transverse steel arrangement. For a given transverse steel arrangement, the equivalent

stiffness of the transverse steel system against buckling can be calculated from the following equation :

$$k_{eq} = \frac{k_t}{(\pi^4 EI/s^3)} \quad (2.24)$$

where

$$k_t = \left(\frac{E_t A_t}{l_e} \right) \left(\frac{n_l}{n_b} \right) \quad (2.25)$$

$$EI = \frac{E_s I}{2} \sqrt{\frac{f_y}{400}} \quad (2.26)$$

In Eq. (2.25), E_t , A_t and l_e are elastic modulus, cross-sectional area and length of transverse steel, respectively while n_l is the number of tie legs along the buckling direction and n_b is the number of longitudinal reinforcements prone to simultaneous buckling. I denotes the moment of inertia of the reinforcement.

Table 2.1 shows the relationship between k_{eq} and the buckling mode, n . By using the value of the equivalent stiffness together with Table 2.1, the unsupported length, L , can be calculated from the following equation:

$$L = ns \quad (2.27)$$

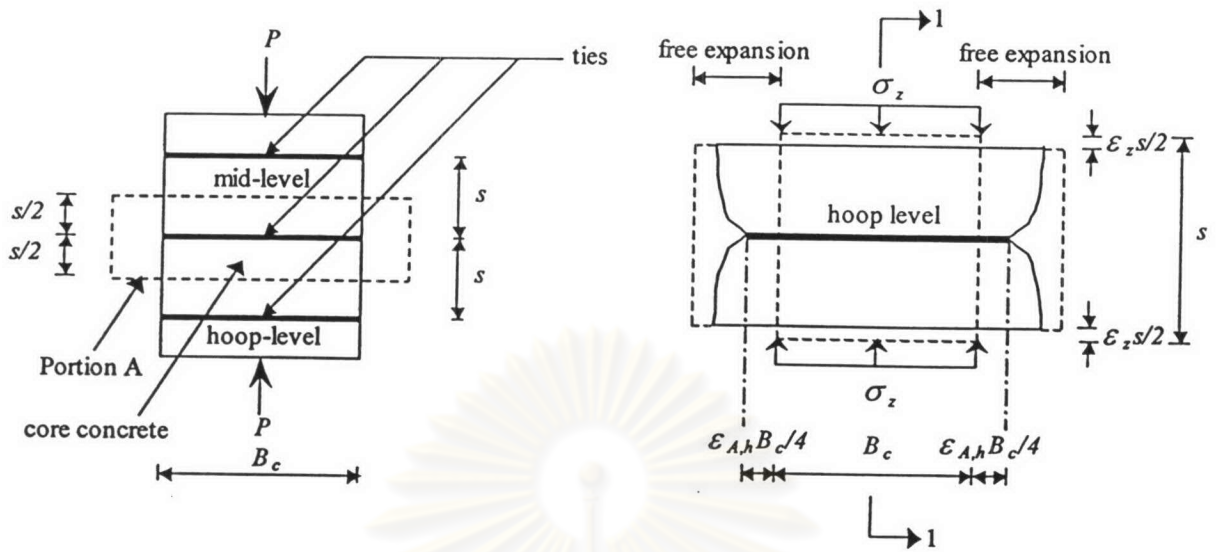


Figure 2.1 (a) Column core under consideration; (b) Deformation of Portion A

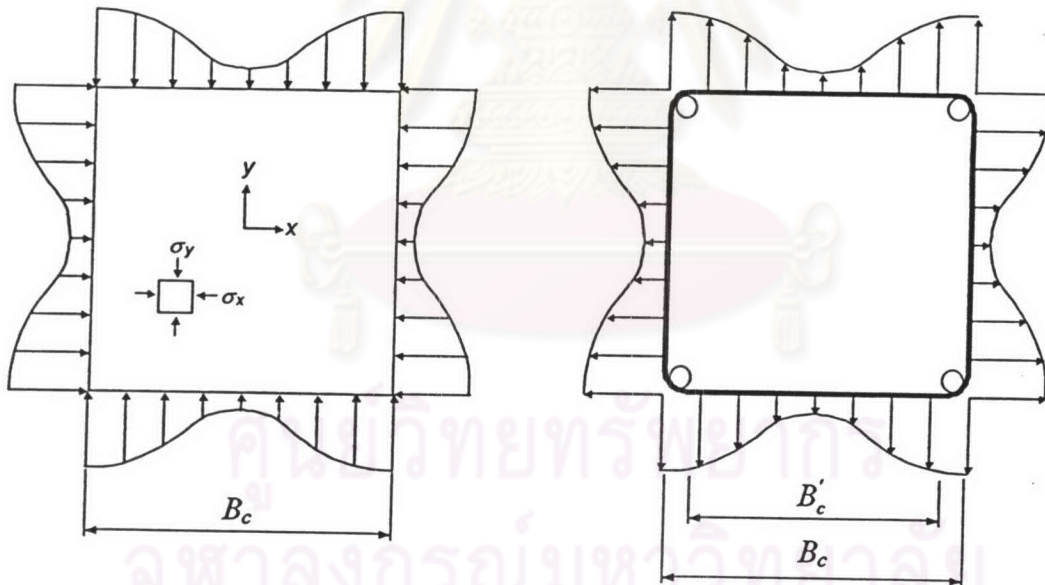


Figure 2.2 Interactive confining forces at hoop level: (a) acting on concrete (b) acting on perimeter tie

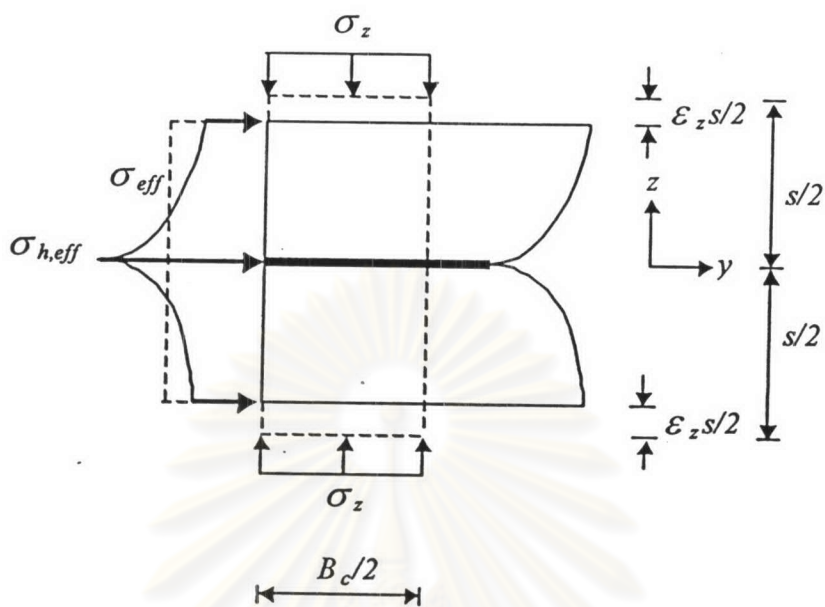


Figure 2.3 Internal stress distribution in the concrete core at section 1-1

ศูนย์วิทยทรัพยากร
จุฬาลงกรณ์มหาวิทยาลัย

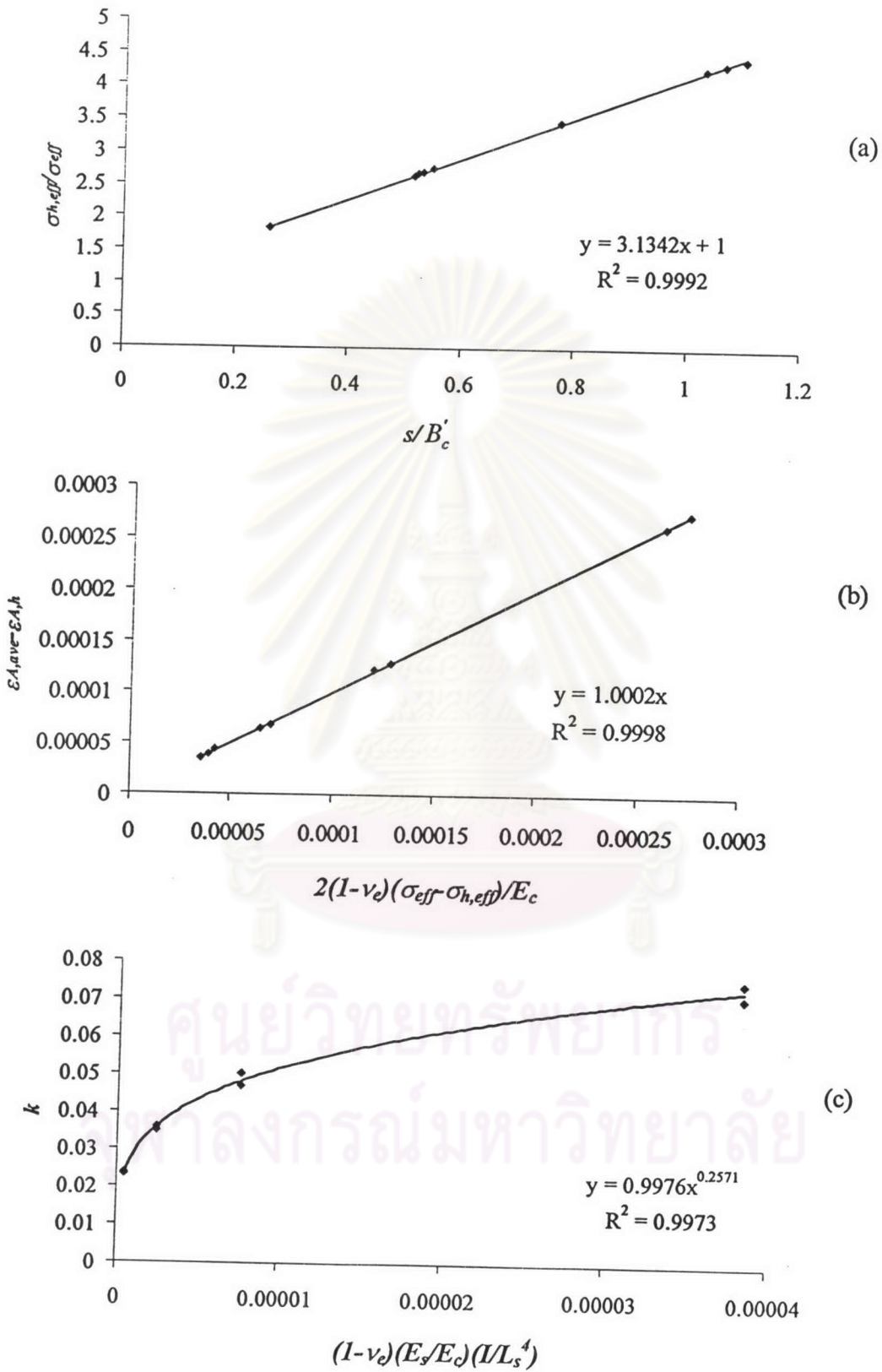


Figure 2.4 Results from finite element analyses

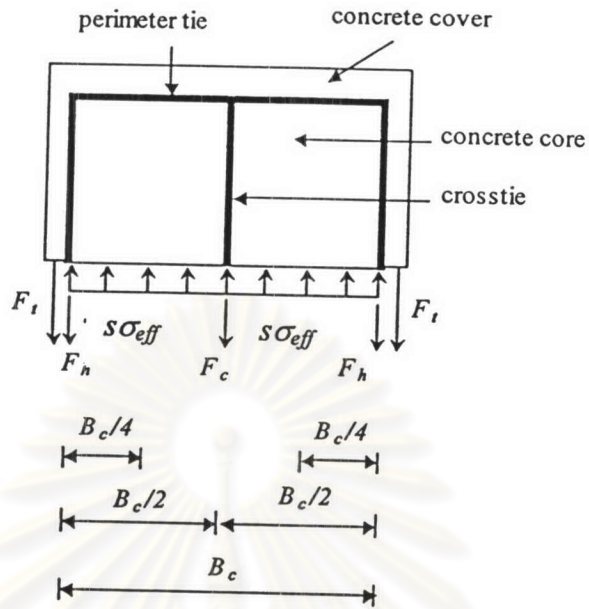


Figure 2.5 Equilibrium condition

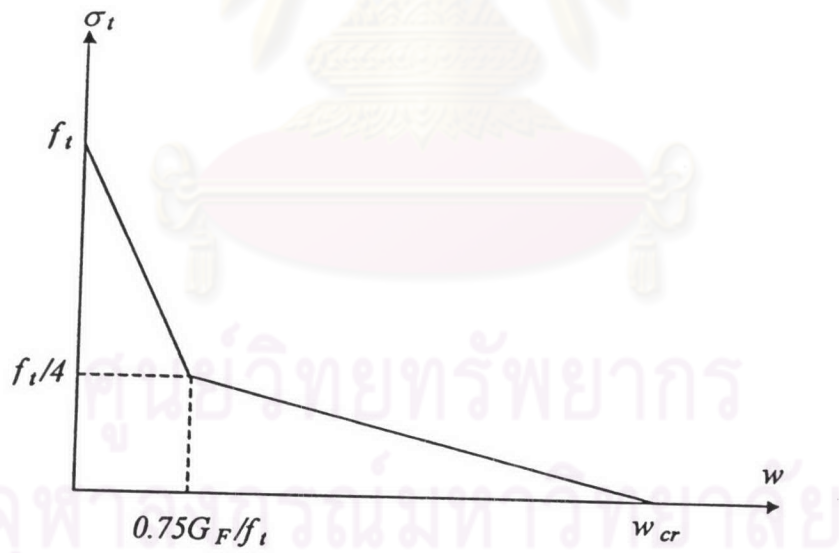


Figure 2.6 Tensile strength-crack width relationship

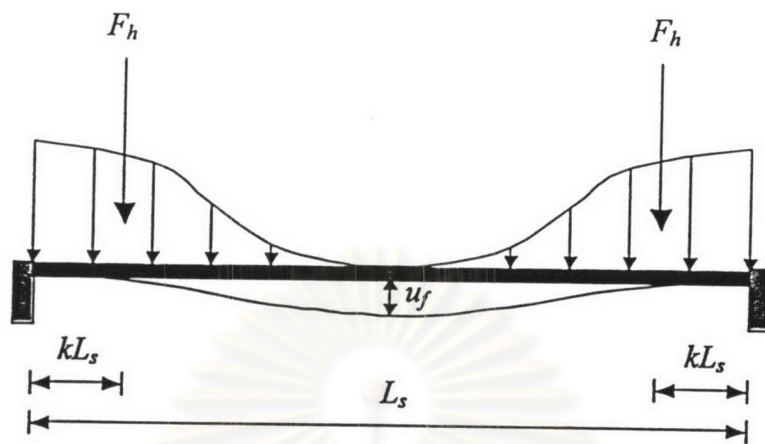


Figure 2.7 Distribution of interactive line forces and resultant forces on part of perimeter tie at transverse restraints

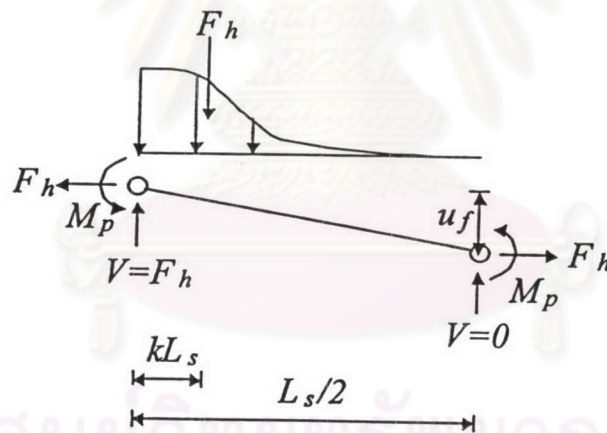


Figure 2.8 Equilibrium condition of hoop leg with two plastic hinges formed at the end supports

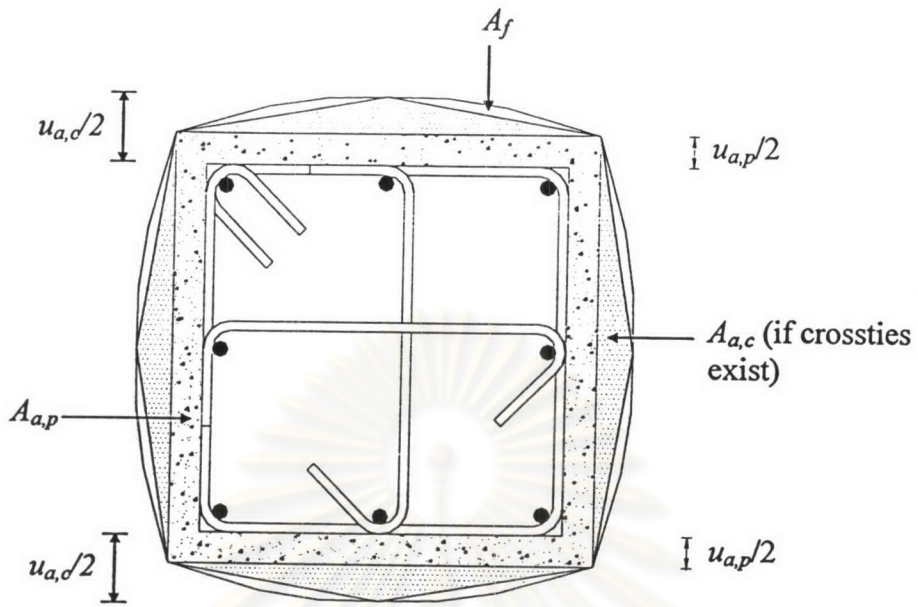


Figure 2.9 Concept of area compatibility

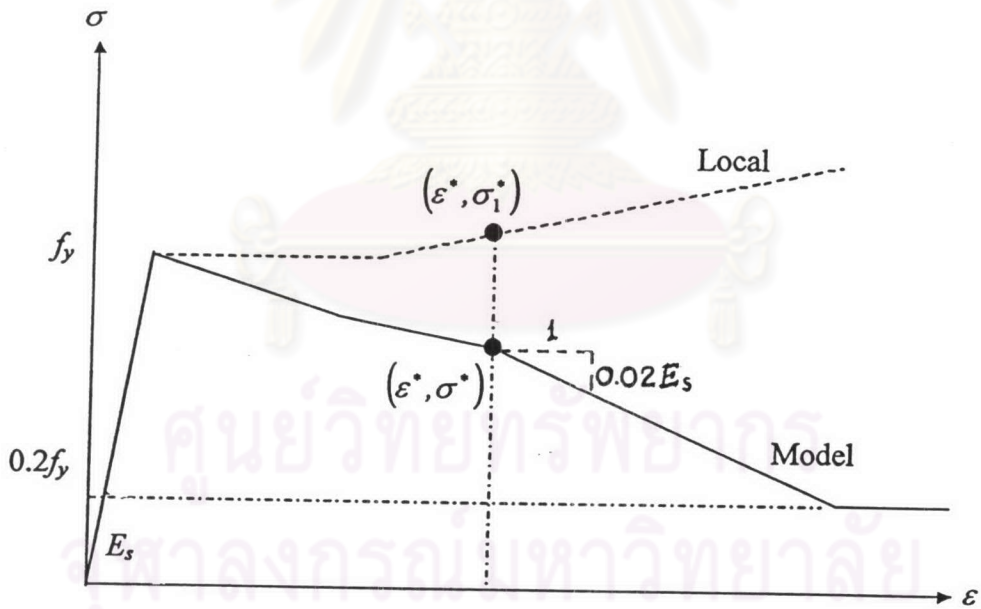


Figure 2.10 Typical stress-strain relation for reinforcement under compression [Dhakar (2000)]

Table 2.1 Required equivalent stiffness for different buckling modes [Dhakal (2000)]

Mode, n	1	2	3	4	5	6	7	8
k_{eq}	0.75	0.1649	0.0976	0.0448	0.0084	0.0063	0.0037	0.0031



ศูนย์วิทยทรัพยากร
จุฬาลงกรณ์มหาวิทยาลัย